Annals of Phytomedicine 13(1): 1259-1269, 2024

DOI: http://dx.doi.org/10.54085/ap.2024.13.1.137

Annals of Phytomedicine: An International Journal
http://www.ukaazpublications.com/publications/index.php

Print ISSN : 2278-9839 Online ISSN : 2393-9885

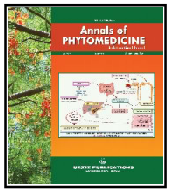

Original Article : Open Access

Catalytic degradation of organic pollutant by biosynthesized silver nanoparticles using *Trigonella foenum-graceum* L. leaves

Monika Moond, Sushila Singh◆, Seema Sangwan*and Rajni Kant Sharma
Department of Chemistry, Chaudhary Charan Singh Haryana Agricultural University, Hisar 125004, Haryana, India
**Department of Microbiology, Chaudhary Charan Singh Haryana Agricultural University, Hisar 125004, Haryana, India*

Article Info

Article history
Received 14 March 2024
Revised 30 April 2024
Accepted 1 May 2024
Published Online 30 June 2024

Keywords
Green synthesis
Silver nanoparticles
Optimized
Morphology
Catalyst

Abstract

The usefulness of plant extracts in the green synthesis of silver nanoparticles (AgNPs) has received considerable interest because it is easy, environmentally benign, stable, and economical. The present study involved the biosynthesis of AgNPs using *Trigonella foenum-graceum* L. leaf extract. The different reaction conditions, such as the amount of leaf extract, temperature, concentration of silver nitrate ($AgNO_3$), pH, and reaction time, were optimized using a UV-Visible spectrophotometer. The average particle size, morphology, and elemental composition of the AgNPs were studied using UV-Vis spectroscopy, Particle size analyser (PSA), Field emission scanning electron microscopy coupled to Energy-dispersive X-ray spectroscopy (FESEM-EDX), X-ray diffraction (XRD), High resolution transmission electron microscopy (HRTEM) and Fourier transform infrared spectroscopy (FTIR). The average size of the AgNPs was 19 nm and they were spherical in shape. The efficacy of AgNPs as a catalyst was confirmed by the 13 min completion of the reduction of the organic pollutant p-nitrophenol (p-NP). The catalytic capabilities of AgNPs strongly support their use for the purification of contaminated water.

1. Introduction

Noble metal nanostructures have recently drawn a lot of attention as a result of the development of nanotechnology and their potential to make significant contributions to the disciplines of renewable energy, plasmonic, catalysis, and photocatalysis (Chen *et al*., 2013; Singh *et al*., 2021; Aggarwal *et al*., 2022; Moond *et al*., 2023). As a result, the technology for developing them has been improved to produce shape, size, and geometry-controlled nanostructures to support various applications. Among metal nanoparticles, silver nanoparticles (AgNPs) have attracted significant interest because of their distinct optical, electronic, and catalytic properties (Singh *et al*., 2018).

A variety of physical and chemical processes can be used to synthesize AgNPs, but doing so may have unintended environmental effects due to the high energy consumption, release of toxic and dangerous chemicals, use of complicated equipment, and synthesis conditions. It is always preferable to use green chemistry as an alternative to conventional methods because of the growing awareness of the detrimental effects of synthetic methods on the environment. As a result, many biological agents, such as plants, bacteria, fungi, and algae, have been reported to synthesize AgNPs on their own without the need for additional stabilizing and reducing agents. The method using plants to synthesize AgNPs is preferable to that using microbes because it is less hazardous to living organisms, versatile, and does not require the maintenance of cell culture (Lee and Jun, 2019; Moond *et al*., 2022; Devi *et al*., 2024). Among the diverse bioreductants, *T. foenum-graceum* leaves were chosen for this study. It is an annual herb also known as Methika (Sanskrit), Greek hay, Fenugreek (English), Kasuri methi, Sag methi (Hindi) and Methi (Marathi) which belong to the family Fabaceae (Moond *et al*., 2023). Due to the existence of numerous bioactive compounds such as apigenin, orientin, luteolin, vitexin quercetin, isovitexin, amino acids, saponins, alkaloids and phenols; it is used to cure a variety of diseases (Poonam *et al*., 2023; Devi *et al*., 2023). These phytochemicals can be utilized as reducing and capping agents for the synthesis of biogenic nanoparticles (Dalal *et al*., 2022; Moond *et al*., 2023).

AgNPs are frequently employed to enhance the catalytic efficiency of reduction processes. They were employed in the one-step reduction of the organic pollutant nitroaromatics to produce amino aromatics. The synthesis of amino aromatics from nitroaromatics is interesting because amino aromatics are crucial building blocks for the synthesis of herbicides, dyes, antioxidants, medicines, polymers, and other fine chemicals (Mejia and Bogireddy, 2022; Singh *et al*., 2018). The catalytic hydrogenation of nitroaromatics using iron, tin, zinc, Au/SiO_2, Au/Al_2O_3, Pd/TiO_2, Pt-Ni bimetallic nanoparticles, and Pt/TiO_2 can easily produce amino aromatics (Marcelo *et al*., 2012). All these processes have drawbacks such as the need for hazardous solvents, potent reducing agents, expensive metals such as Pt, Au, and Pd, heat, high pressure, and the production of hazardous byproducts. However, using AgNPs to reduce nitroaromatics is far superior to any of these other methods because it is less expensive, non-toxic, produces no dangerous byproducts, and only requires ambient temperature and pressure (Deka *et al*., 2017). The toxic and persistent organic pollutant p-nitrophenol has caused widespread concern because of its negative effects on human health. This causes contamination of the surface and groundwater. Consequently, the

Corresponding author: Dr. Sushila Singh
Assistant Professor,Department of Chemistry, CCS Haryana Agricultural University, Hisar-125004, Haryana, India
E-mail: singhsushila999@gmail.com
Tel.: +91-8199939339

water becomes contaminated. The conversion of p-nitrophenol to p-aminophenol has become a crucial issue because p-aminophenol (p-AP) has a lower degree of toxicity (Achamo and Yadav, 2016).

In this study, we synthesized silver nanoparticles (AgNPs) using *T. foenum-graceum* leaf extract by optimizing the reaction conditions such as the amount of extract, concentration of silver nitrate ($AgNO_3$), temperature, pH of the reaction medium, and reaction time. These nanoparticles were characterized by UV-visible spectroscopy, particle size analyser (PSA), Field emission scanning electron microscopy coupled to Energy-dispersive X-ray spectroscopy (FESEM-EDX), X-ray diffraction (XRD), High resolution transmission electron microscopy (HRTEM), and Fourier transform infrared spectroscopy (FTIR). Additionally, the catalytic activity of AgNPs for the reduction of the organic pollutant p-nitrophenol to p-aminophenol was evaluated.

2. Materials and Methods

2.1 Chemicals and collection of plant material

Himedia Private Limited supplied the silver nitrate (CAS No. 7761-88-8), Sodium borohydride (CAS No. 16940-66-2) and p-nitrophenol (CAS No. 100-02-7). *Trigonella foenum-graceum* L. leaves were acquired from the Vegetable Science Research Farm at Chaudhary Charan Singh Haryana Agricultural University. The collected sample was verified by Dr. Anita, Asstt. Scientist, Department of Botany and Plant Physiology, CCS HAU, by using online platform (Tropicos & IPNI LSID: 523957-1). Leaves were cleaned, and then dried at room temperature in the shade.

2.2 Preparation of aqueous leaves extract

70 ml of deionized water and 5 g of powdered dried leaves were heated at 60°C for 30 min. The leaves extract was centrifuged for 25 min at 9500 rpm after filtering with Whatman Filter Paper No. 1 and then stored at 4°C for further research.

2.3 Synthesis of silver nanoparticles (AgNPs) using aqueous leaves extract

For the synthesis of AgNPs, the reaction parameters, including the quantity of extract, temperature, concentration of $AgNO_3$, pH of the reaction medium, and incubation time, were optimized. The synthesis was performed under ideal circumstances: 0.2 ml of aqueous leaves extract was added to 25 ml of $AgNO_3$. The reaction mixture was then stirred for 60 min at 45^0C. Instantaneously, the light-yellow colour of the reaction mixture turned dark brown. The reduction reaction was complete after the reaction mixture was incubated for 24 h. Subsequently, no additional colour change was observed. The reaction mixture was centrifuged for 20 min at 12,000 rpm to precipitate AgNPs. The AgNPs were then dried in an oven and used for further experiments (Moond *et al*., 2023).

2.4 Characterization of silver nanoparticles (AgNPs)

The surface plasmon resonance (SPR) band of the synthesized AgNPs was confirmed using a UV-Vis spectrophotometer (Model UV 1900, Shimadzu). Using particle size analyzer (Microtrac Nanotracwave II), the polydispersity index (PDI) and hydrodynamic diameter of the nanoparticles were determined. To analyze the surface morphology and elemental composition of AgNPs, a field emission scanning electron microscope (FESEM, JSM-7610FPlus) with an energy-dispersive X-ray spectroscopy (EDX) detector was utilized. The crystallinity, phase composition, and purity of the nanoparticles were evaluated by X-ray diffraction (XRD) on a Miniflex II desktop X-ray diffractometer with Ni-filtered Cu Kα radiation (λ = 1.5418 A^0) in the 2θ range of 10-80 at a scanning rate of 0.020/s. High-resolution transmission electron microscopy (JEM/2100 PLUS operating at 200 kV) was used to examine the morphology of nanoparticles. An FTIR spectrophotometer (Perkin Elmer) was used to obtain FTIR spectra (Moond *et al*., 2023; Sooraj *et al*., 2021).

2.5 Catalytic reduction of p-nitrophenol to p-aminophenol

To evaluate the catalytic activity of biosynthesized AgNPs, 0.01M aqueous solution of p-nitrophenol (p-NP) and 0.1 M solution of sodium borohydride ($NaBH_4$) were prepared. The absorbance of 40 µl of aqueous solution p-NP (0.01M) was determined using a UV-Vis spectrophotometer after being diluted up to 3 ml. A freshly made 0.2 ml of sodium borohydride (0.1M) aqueous solution was mixed with an aliquot of 40 µl of p-NP solution (0.01M), which was then diluted with deionized water to make a volume of 3 ml. The absorbance of this mixture was then determined. Lastly, 30 µl of AgNPs were added to the aforementioned reaction mixture and vigorously shaken. UV-Vis spectrophotometer measured the progress of the reaction. The concentration of sodium borohydride could be thought of as constant throughout the reaction because it was greater than the concentration of p-NP. The concentration of p-NP had an impact on the reaction rate, and as a result, the reaction followed pseudo first-order kinetics. A plot of ln (A/A_0) as a function of time was created to study the reaction's kinetics, and the rate constant's value was determined (Chen *et al*., 2008).

$$\ln C/C_0 = \ln A/A_0$$

where, C_0 is the initial concentration, C is the concentration at time t, similarly A_0 is initial absorbance and A is absorbance at time t.

3. Results

3.1 Optimization of biosynthesis of AgNPs using UV-Vis spectroscopy analysis

3.1.1 Effect of leaves extract amount

Biosynthesis of AgNPs was performed by varying amount of leaf extract (0.1, 0.2, 0.3, 0.4 and 0.5 ml) in 25 ml of a 1mM $AgNO_3$ solution at room temperature and neutral pH. With an increase in the ratio of leaf extract to $AgNO_3$ solution (above 0.2 ml), surface plasmon resonance (SPR) band became broader (Figure1). This can be explained by the presence of many reductants in the reaction medium, which accelerated the reduction of Ag^+ ions. By a process known as Ostwald ripening, which results in an increase in nanoparticle size, the quick reduction of Ag^+ ions typically facilitating further growth of nanoparticles. At concentration ratio $AgNO_3$: leaves extract 25:0.2 (ml: ml) a sharp band at λ_{max} 448 nm was observed. Upon increasing the concentration beyond 0.5 ml, it was found that within two hours, the color of the solution turned blackish grey and the formation of AgNPs was restricted. Based on the above observation, 0.2 ml was found to be the appropriate amount for the synthesis of AgNPs.

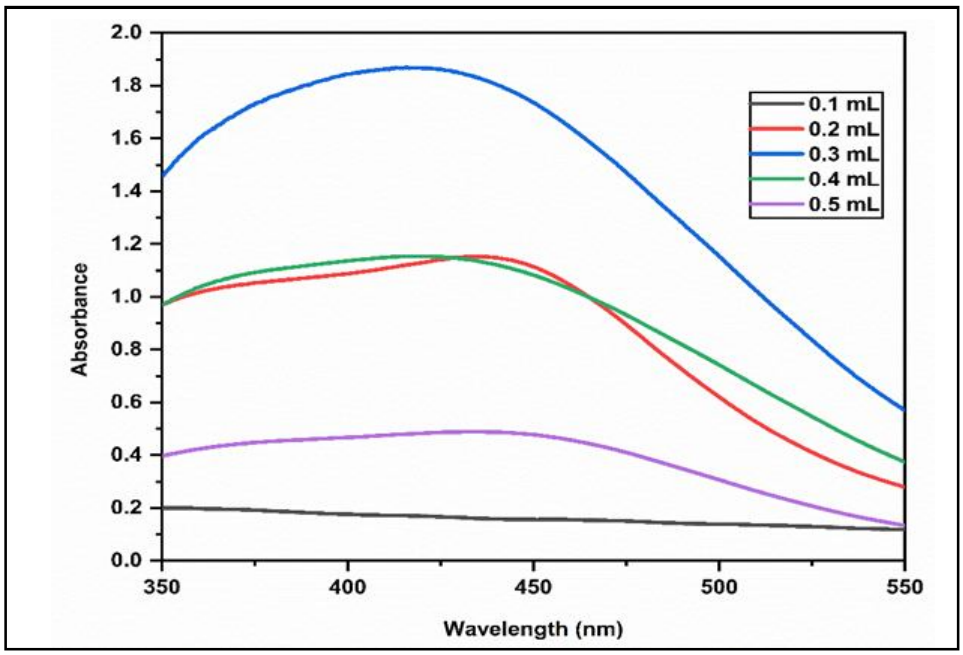

Figure 1: UV-Vis spectra showing effect of varying amount of extract on biosynthesis of AgNPs.

3.1.2 Effect of silver nitrate concentration

Biosynthesis of AgNPs usingleaf extract was performed by varying $AgNO_3$ (25 ml) concentrations (0.5, 1.0, 2.0, 3.0 and 5.0 mM) with 0.2 ml leaves aqueous extract at room temperature and neutral pH. From the UV-Vis data, it can be concluded that no AgNPs at 0.5 mM concentration of $AgNO_3$. An intense, sharp and characteristic SPR band was observed for 1 mM $AgNO_3$ solution. The SPR band broadened and shifted slightly towards longer wavelengths (red-shift) after 1 mM, indicating an increase in the size of the synthesized AgNPs. This increase in size may be caused by the secondary reduction of silver ions that were adsorbed on the surface of the built nuclei at higher Ag^+ concentrations, resulting in the generation of larger nanoparticles (Figure 2). Beyond 1mM, it was observed that agglomeration of particles started within 1 h of synthesis, probably because of the insufficient amount of capping agent present in the plant extract to stabilize the biosynthesized AgNPs. At 5 mM $AgNO_3$, agglomeration was clearly observed. Therefore, 1 mM $AgNO_3$ was chosen for the synthesis of AgNPs.

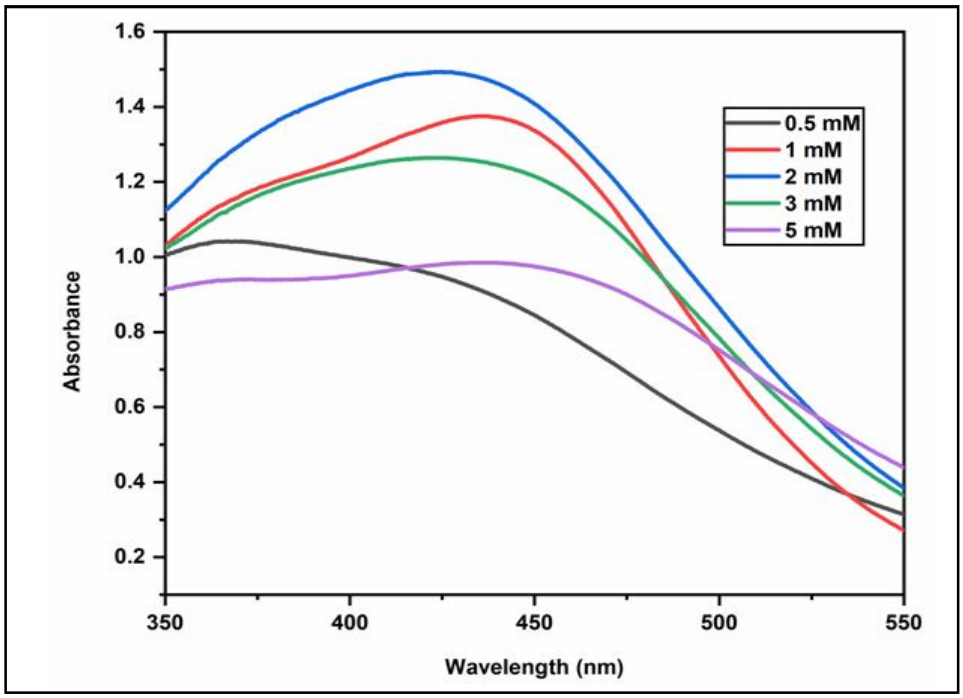

Figure2: UV-Vis spectra showing effect of varying concentration of $AgNO_3$ on biosynthesis of AgNPs.

3.1.3 Effect of temperature

Biosynthesis of AgNPs using leaf extract was performed at various temperatures (room temperature, 45ºC, 60ºC, 70ºC and 80ºC) with 0.2 ml leaves extract in 25 ml of 1 mM $AgNO_3$ solution at neutral pH for 60 min. The intensity of the absorption peak increases with increasing temperature. The time required for the biosynthesis of AgNPs decreased with increasing temperature because of an increase in the kinetic energy of the reaction mixture. At 45°C, a blue shift was observed, indicating a smaller size of the synthesized AgNPs. Further temperature rise was accompanied by an increase in peak broadness and a decrease in SPR intensity, indicating that the reducing and stabilising properties of the leaf extract decreased at higher temperatures (Figure 3). Keeping in view, that the stability of plant metabolites present in the reaction mixture requires working at ambient temperature, 45°C was chosen as the optimum temperature for the synthesis of AgNPs.

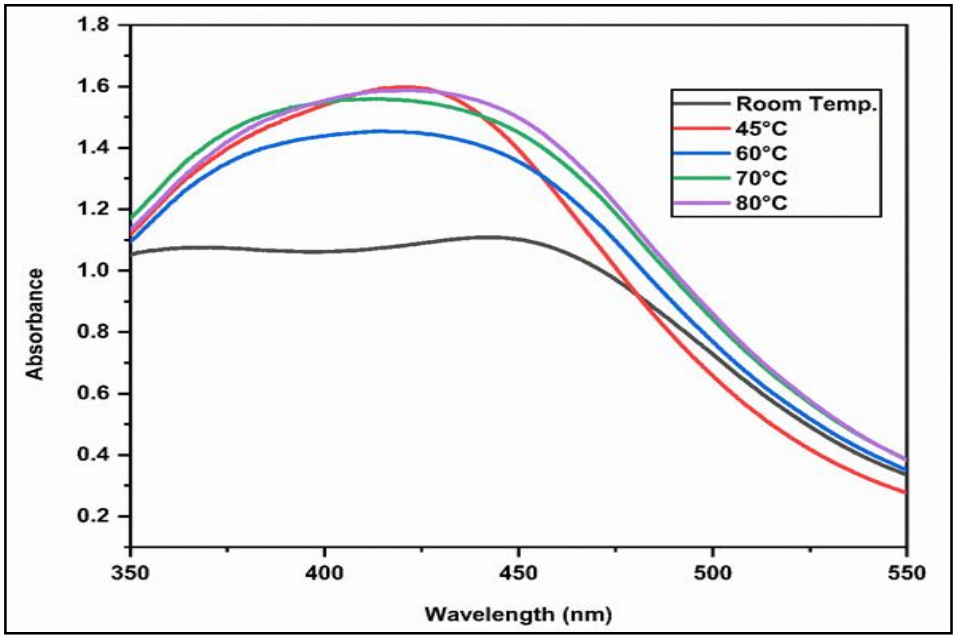

Figure 3: UV-Vis spectra showing effect of reaction temperature on biosynthesis ofAgNPs.

3.1.4 Effect of pH

Biosynthesis of AgNPs using the leaf extract was performed by varying the pH (3, 5, 7, 9, and 11) with 0.2 ml extract in 25 ml of 1 mM silver nitrate at room temperature. The initial pH of the $AgNO_3$ solution plays an important role in the synthesis of AgNPs. From the UV-Vis spectra (Figure 4), it can be seen that, with an increase in the pH of the metal salt solution, the intensity of the SPR band increased. This shift in the absorbance maxima clearly indicated that the size of the AgNPs decreased when the pH of the solution was changed from 3 to 7 (acidic to neutral). Upon further increasing the pH from 7 to 11 (from neutral to basic), agglomeration was observed after 2 h. The optimum pH for nanoparticles synthesis was chosen to be pH 7.

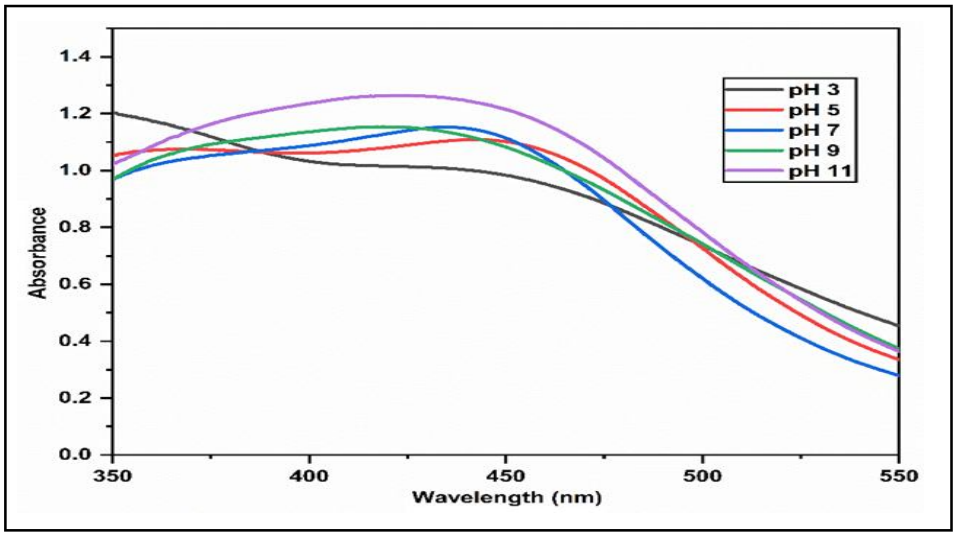

Figure 4: UV-Vis spectra showing effect of pH on biosynthesis of AgNPs.

3.1.5 Effect of reaction time

At room temperature, 0.2 ml extract in 25 ml of 1 mM silver nitrate at neutral pH and varying reaction duration from 1 h to 24 h was used for the biosynthesis of AgNPs. The UV-Vis spectra of the reaction media at different time intervals (1-24 h) are shown in Figure 5. From the spectra, it can be observed that no significant or very low reduction in the reaction media occurred in the first 1 h of the reaction. The intensity of the SPR band increased with time and became almost constant after 24 h of incubation. An intense reddish-brown color was observed at the end of the reaction. A plot of maximum absorbance versus time revealed that there was an increase in absorption from 1 h to 24 h, but thereafter, there was no significant change in maximum absorbance, which indicated that reduction had been completed. The optimized reaction conditions for the biosynthesis of AgNPs using aqueous leaf extracts are listed in Table 1.

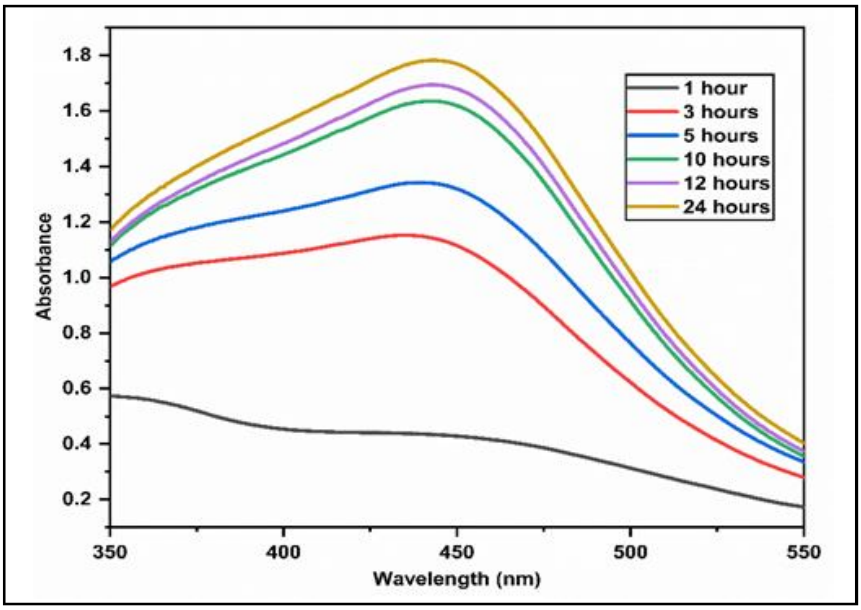

Figure 5: UV-Vis spectra showing effect of reaction time on biosynthesis of AgNPs.

Table 1: Optimized reaction conditions for biosynthesis of AgNPs by using aqueous leaves extract

Optimization of reaction conditions	Corresponding values
Reaction conditions	Dark
Fenugreek leaves extract amount	0.2 ml
$AgNO_3$ concentration	1mM
Temperature	45°C
pH of the medium	7
Reaction time	24 h

3.2 Characterization of biosynthesized AgNPs

3.2.1 UV-visible spectroscopy

The chemical reaction between the dissolved silver ions and the leaf extract was investigated using a UV-visible spectrophotometer. AgNPs were formed upon completion of the reduction reaction. Owing to the surface plasmon resonance phenomenon (Bahuguna *et al*., 2016), UV-visible analysis revealed an absorption peak at 440 nm, as shown in Figure 6.

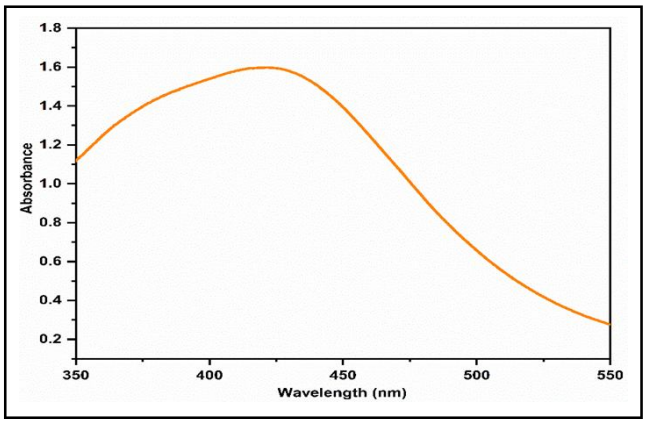

Figure 6: UV-Vis absorption spectra of AgNPs.

3.2.2 Particle size analyser

The PSA size distribution of AgNPs is shown in Figure 7. The polydispersity index (PDI) and hydrodynamic diameter of AgNPs was 0.24 and 63 nm, respectively.

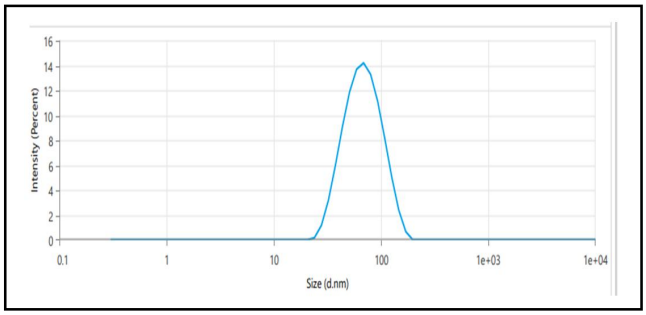

Figure 7:PSA of biosynthesized AgNPs.

3.2.3 FESEM-EDX analysis

FESEM analysis was performed to investigate the surface morphology and chemical composition of the biosynthesized AgNPs. The biosynthesized AgNPs were found to be mostly spherical with an average size of 19 nm (Figure 8). Energy-dispersive X-ray spectroscopy (EDX) was performed to determine the elemental composition of the nanoparticles (Table 2).

EDX analysis of AgNPs showed metallic silver (19.71 %) along with other elements such as carbon (19.99 %), oxygen (59.40%), and chlorine (0.90 %).

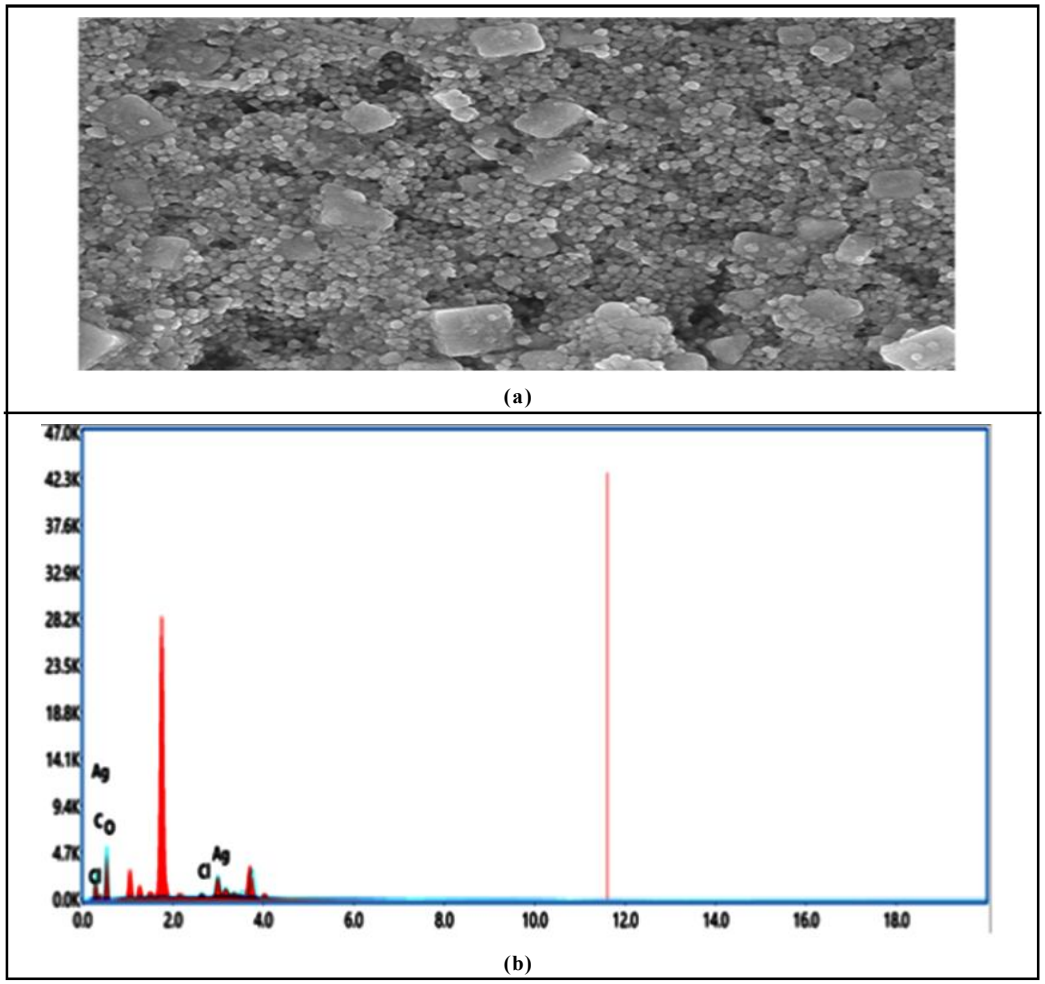

Figure 8: FESEM micrograph (a) 100 nm scale (b) elemental mapping of AgNPs.

Table 2: EDX analysis parameters of AgNPs

Element	Weight %	Atomic %
Carbon	19.99	29.80
Oxygen	59.40	66.48
Silver	19.71	3.27
Chlorine	0.90	0.45

3.2.4. XRD

The XRD diffraction pattern of AgNPs showedsharp peaks at 2θ (38.18º, 44.84º, 64.68º and 77.65º) corresponding to the (111), (200), (220) and (311) Bragg reflections, respectively (Figure 9). These reflections were similar to those reported for the FCC lattice structure of standard Silver (Ag) metal and were consistent with the standard data file ICSD No. 98-004-4387. The high intensity peak at 38.18º indicated a high level of crystallinity and the (111) plane was the predominant orientation (Umadevi *et al*., 2013).

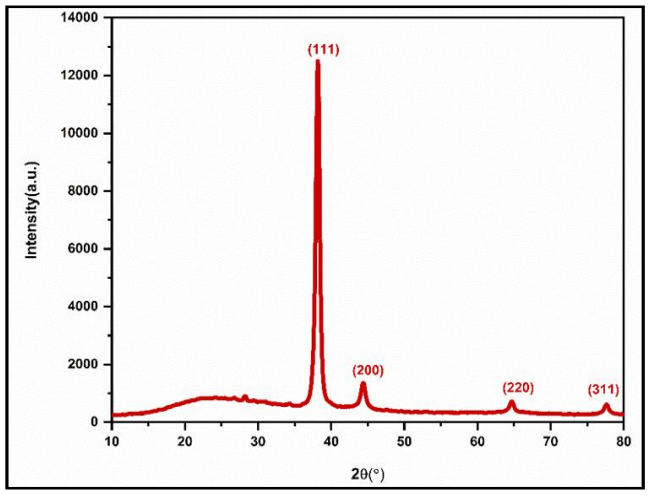

Figure 9: XRD of biosynthesized AgNPs.

3.2.5 HRTEM

The morphology and size of the green-synthesized AgNPs were evaluated using HRTEM analysis. HRTEM images showing the presence of AgNPs at 20 nm and 50 nm magnifications are shown in Figure 10a and 10b, respectively. The synthesized AgNPs were spherical with an average size of 19 nm.

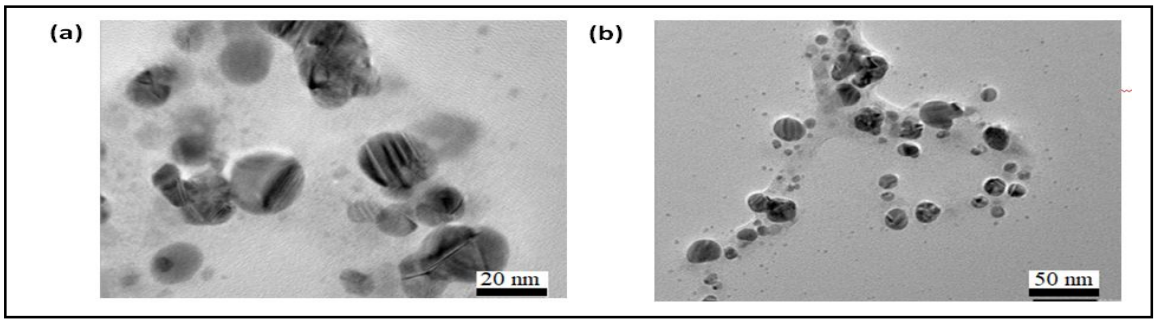

Figure 10: Images of HR-TEM showing the presence of AgNPs recorded at (a) 20nm (b) 50nm magnification levels.

3.2.6 FTIR

FTIR analysis was performed to identify the various functional groups in the leaf extract and on the surface of the biosynthesized AgNPs that were primarily responsible for the reduction of silver nitrate (Ag^+ to Ag) and the stabilization of AgNPs. Figure 11 depicts the FT-IR spectra of the seed extract and biosynthesized AgNPs. Analysis of the FT-IR spectra of leaves revealed the presence of various characteristic peaks at 3321, 2947, 2835, 1653, 1448, and 1011 cm^{-1}, and the biosynthesized AgNPs also showed peaks at 3337, 2924, 1645, 1432, and 1010 cm^{-1} (Table 3). The similarity between these two spectra with some marginal shift in the peak positions confirmed that AgNPs were capped with various phytochemicals in the leaf extract (Moond *et al*., 2023).

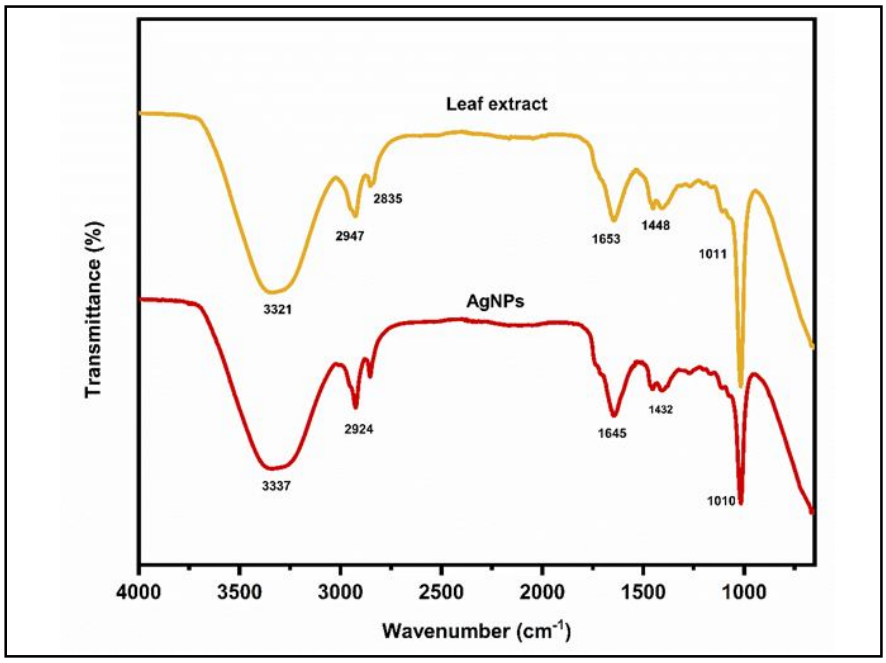

Figure 11: Comparative FTIR spectra of leaves extract and their biosynthesized AgNPs.

Table 3:Assignment of various peaks observed during FTIR analysis

Entity	Observed wavenumber (cm^{-1})	Assignment of peaks	Range (cm^{-1})
1.	3321, 3337	O-H stretch, N-H stretch,intermolecular H-bonding	3200-3500
2.	2924, 2947, 2835	C-H stretch	2700-2950
3.	1645, 1653	-C=O stretch	1650-1850
4.	1448, 1432	stretching vibration of alkenes CP%C in aromatic rings	1380-1465
5.	1010,1011	C-O stretch, C-N stretch	1015-1250

3.3 Evaluation of catalytic activity

The reduction of the organic pollutant p-nitrophenol to p-aminophenol using aqueous $NaBH_4$ is a thermodynamically favourable reaction (E_0 for p-nitrophenol/p-aminophenol -0.76 V and for H_3BO_3/BH_4 -1.33 V), but kinetically unfavourable because of the large potential difference between the donor and acceptor species (Kong *et al*., 2017). In the reaction of aqueous solution of p-NP (0.01M) with a freshly prepared aqueous solution of $NaBH_4$ (0.1 M), a redshift from 319.4 nm to 402 nm was observed due to the formation of 4-nitrophenolate ions (Figure 12). Moreover, by adding 30 µl of colloidal AgNPs to the reaction mixture, a rapid lowering of the absorption peak at 402 nm was observed with synchronal formation of a new peak at 300 nm, thus indicating the formation of p-aminophenol. Complete disappearance of the 402 nm peak was observed within 13 min, thus indicating the completion of the reduction reaction by showing the catalytic activity of biosynthesized AgNPs. Pseudo first-order rate kinetics can be applied to the reduction reaction as the concentration of the BH_4^- was much higher than p-NP (Kastner and Thunemann, 2016). The reaction rate constant (k) is 0.1398 min^{-1}.

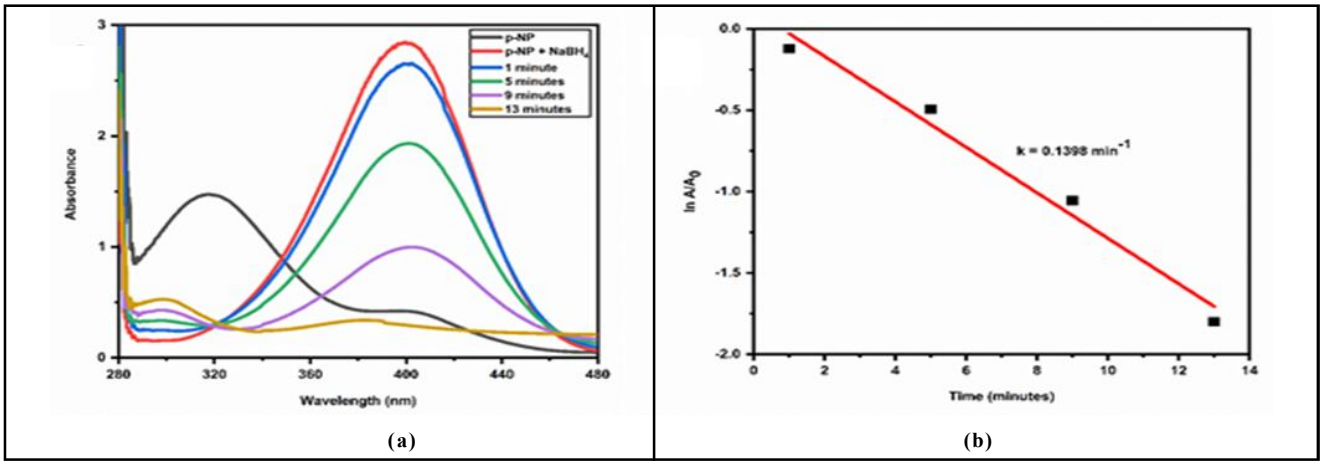

Figure 12: (a) Time dependent UV-vis spectra for the reduction of p- nitrophenol (p-NP) by $NaBH_4$ catalyzed using AgNPs (b) plot of ln[*A*] vs time for the reduction of p-NP using AgNPs.

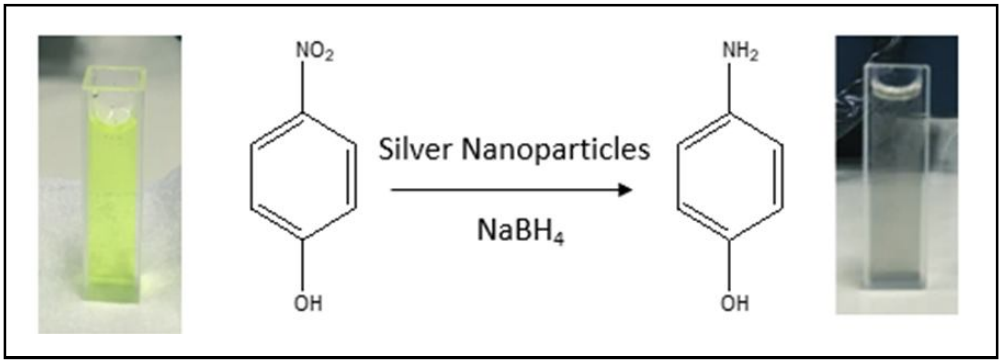

Figure13: Reduction reaction of p-nitrophenol to p-aminophenol.

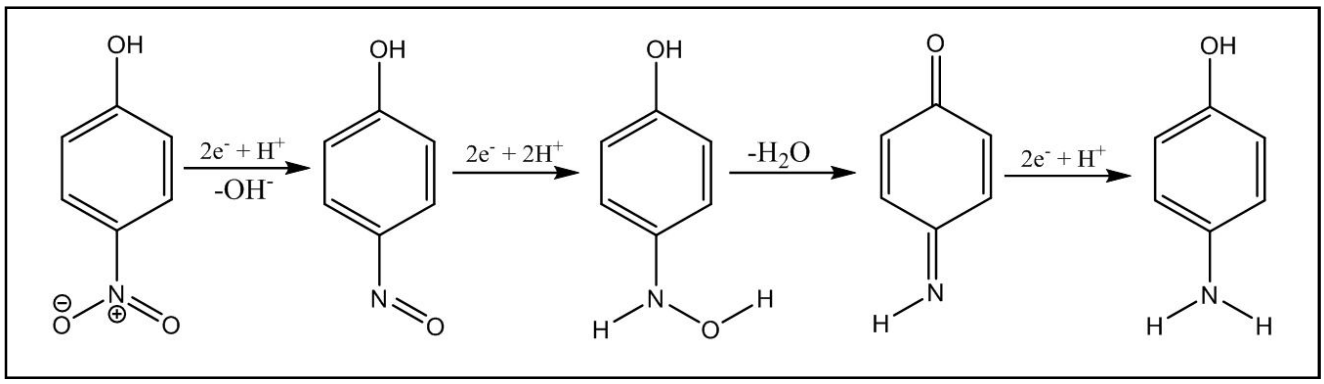

Figure 14: Possible reaction mechanism for conversion of p-nitrophenol to p-aminophenol.

4. Discussion

4.1 Optimization of biosynthesis of AgNPs

The reduction of silver ions, clustering, and subsequent nanoparticle growth are the three major steps in the mechanism of AgNPs production. The characteristics of each phase depend on the amount of the reducing agent, concentration of silver nitrate, temperature, pH and reaction time (Makarov *et al*., 2014). The effect of fenugreek leaf extract (0.1, 0.2, 0.3, 0.4 and 0.5 ml) on the biosynthesis of AgNPs was investigated. A sharp peak was obtained with 0.2 ml of Fenugreek leaves extract, which was chosen as the optimized parameter for analysis. Similar results were obtained by other researchers. Jain and Mehata (2017) studied the effect of the amount of leaf extracts of *Ocimum sanctum* (Tulsi) on the formation of AgNPs by mixing 2 mM $AgNO_3$ solution and Tulsi leaf extract in different amounts. A red shift of the absorption band towards a longer wavelength (430-450 nm) was observed with increasing amounts of the leaf extract, indicating that the particle size increased with increasing amounts of leaf extract.

The effect of silver nitrate concentration was optimized by measuring the absorption spectra of the reaction mixture containing fenugreek leaf extract (0.2 ml) and various concentrations of silver nitrate (0.5, 1, 2, 3, and 5 mM) at room temperature and neutral pH. A sharp peak was obtained with 1 mM fenugreek leaf extract, which was chosen as the optimized parameter for analysis. Our findings match the results of Mahiuddin *et al.* (2020), who biosynthesized AgNPs using an aqueous extract of *Piper chaba* stems at different concentrations of silver salt (0.5 to 10 mM) at pH 7 and revealed that 1mM concentration of $AgNO_3$ was the optimum concentration for the synthesis of AgNPs of desirable size.

The effect of temperature (room temperature-80^{0}C) on the synthesis of AgNPs was studied using fenugreek leaf (0.2 ml) aqueous extract in silver nitrate (1 mM) at neutral pH. The results of the present study suggested that 45ºC was the optimum temperature for obtaining high-quality AgNPs. Jain and Mehata (2017) revealed that the reaction temperature has a significant effect on the size and morphology of the synthesized AgNPs. The effect of temperature on the formation of AgNPs using Tulsi leaf extract was studied by varying the temperature from 5°C to 35°C and observing that smaller particles with nearly uniform size distribution were formed at higher temperatures.

A wide pH range (3-11) was studied during the biosynthesis of AgNPs using fenugreek leaf aqueous extract (0.2 ml) in 1 mM $AgNO_3$ solution. The results of the present study suggested that pH 7 is the optimum pH for AgNPs biosynthesis. Similar results have been previously reported. Samari *et al.* (2018) optimized the pH of reaction mixture (pH 3-11) for the synthesis of AgNPs using mango leaf extract. The results revealed that at pH 7, the formation of AgNPs was instantaneous, and an intense SPR band was observed owing to the ionization of the phenolic groups present in the leaf extract.

The effect of reaction time on the rate of reduction and stability of biosynthesized AgNPs was investigated under optimized conditions of fenugreek leaf (0.2 ml) aqueous extract and silver salt concentration (1mM) at neutral pH and 45ºC. The maximum absorbance of the reaction mixture was observed after 24 h of incubation, indicating almost complete reduction of Ag^+ to Ag. Satishkumar *et al.* (2010) demonstrated the importance of reaction time in controlling the size of AgNPs. TEM images of AgNPs synthesized using *Curcuma longa* tubers showed that the size of the formed AgNPs was smaller in the initial 24 h than in the subsequent 168 h of the bioreduction experiment.

4.2 Characterization of biosynthesized AgNPs

Biosynthesized AgNPs using fenugreek leaf aqueous extracts of different sizes, shapes and morphologies were characterized by using various techniques. The biosynthesized AgNPs showed a characteristic absorption peak in the UV-Vis spectrum at 440 nm using fenugreek leaf extract. Awad *et al.* (2021) synthesized AgNPs using *T. foenum-graecum* seed extract and characterized using UV-Vis spectroscopy which showed a maximum absorption peak at 443 nm.

PSA measures the hydrodynamic diameter of synthesized AgNPs in a reaction mixture that includes the entire thickness of the layer of capping or reducing agents adsorbed on the surface of the nanoparticles (Kumar *et al*., 2016). The polydispersity index (PDI) and hydrodynamic diameter of AgNPs using PSA was 0.24 and 63 nm respectively. Singh *et al.* (2011) synthesized AgNPs using leaf extract of Fenugreek by chemical reduction and reported an average size of 48.07 nm measured using PSA after 8 days of reaction.

FESEM coupled with EDX and elemental mapping were used to study the surface morphology and chemical composition of the biosynthesized AgNPs. The biosynthesized AgNPs were found to be mostly spherical with an average size of 19 nm. The optical absorption peak at 3.0 KeV confirmed the presence Ag and signals observed for C, O and Si can be attributed to the organic substances found in the plant extract. In the FESEM analysis, the coexistence of small sized and large sized nanoparticles was caused by their time variation in formation during synthesis, which revealed that new nanoparticle formation and aggregation occurred simultaneously. Rizwana *et al.* (2021) reported that the EDX of synthesized AgNPs using Fenugreek leaves exhibited strong signals in the silver region, and an absorption peak was observed at 3 keV.

The XRD diffraction pattern of AgNPs showed sharp peaks at 2θ (38.18º, 44.84º, 64.68º and 77.65º) corresponding to the (111), (200), (220) and (311) Bragg reflections, respectively. The XRD results of the present study match those of Deshmukh *et al.* (2019). Aqueous seed extracts of Fenugreek were used to synthesize AgNPs, which exhibited XRD with 2θ values of 38.1º, 44.4º, 64.4º and 77.3º sets of lattice planes, which were indexed to the (111), (200), (220) and (311) face cantered cubic structure of silver, respectively.

The morphology and size of the AgNPs synthesized using fenugreek leaf extract were examined by HRTEM, revealing spherical nanoparticles with an average size of 19 nm. The morphology and size of AgNPs synthesized using mango leaves extract were determined using TEM and revealed that the AgNPs were almost spherical in shape with size ranged from 14 to 28 nm with an average size of 20.7 nm (Samari *et al*., 2018).

FTIR spectral analysis was performed to evaluate the different types of functional groups of plant extracts that were responsible for capping and stability of biosynthesized AgNPs. These results are in agreement with the findings of other researchers. Deshmukh *et al.* (2019) FTIR studies of AgNPs synthesized using Fenugreek seed extract revealed that amino acids, peptides and proteins can bind with metal, cap the particles and stabilize the nanoparticles against agglomeration.

4.3 Evaluation of catalytic activity

The reduction of p-nitrophenol to p-aminophenol was achieved by adding 30 µl of silver nanoparticles (AgNPs) to a reaction mixture comprising a newly prepared solution of p-NP and $NaBH_4$. The complete vanishing of the peak at 402 nm (4-nitrophenolate ion) was observed in 13 min. The rate constant for this reaction was calculated to be 0.1398 min^{-1}. The reduction of p-nitrophenol to p-aminophenol is illustrated in Figure 13. Using the probable reaction mechanism shown in Figure 14, the catalytic reduction of p-NP by $NaBH_4$ and the metal catalysts was explored. When $NaBH_4$ is ionised in the liquid phase, borohydride ions (BH_4^-) are produced, which bind to the metal catalyst surface to form a metal hydride complex and p-nitrophenol simultaneously adheres to the surface of the metal hydride complex. The synthesis of p-nitrophenolate ions (p-NP) is facilitated by the transfer of H_2 from the hydride complex surface to the p-NP because of the thermodynamic equilibrium on the hydride complex surface (Sen *et al*., 2013). AgNPs initiated the efficient transfer of electrons from the donor BH_4^- ion to the acceptor p-nitrophenolate ion, thereby reducing the activation energy of the reaction (Pei *et al*., 2017).

5. Conclusion

Silver nanoparticles were synthesized using aqueous *Trigonella foenum-graceum* leaf extract, which acts as both a reducing and capping agent. Various reaction conditions, such as the amount of leaf extract, concentration of $AgNO_3$, pH of the reaction medium, temperature, and reaction time, were optimized for the synthesis of AgNPs. Spectroscopic techniques, including UV-Visible Spectroscopy, PSA, FESEM-EDX, XRD, HRTEM, and FTIR were used to characterize AgNPs. These AgNPs have also been employed as catalysts for the conversion of p-nitrophenol to p-aminophenol. The catalytic degradation of the organic pollutant p-nitrophenol in wastewater treatment has received much attention because it is an anthropogenic contaminant that might have a harmful impact on aquatic species.

Acknowledgements

The Department of Chemistry at Chaudhary Charan Singh Haryana Agricultural University, Hisar, provided the necessary resources, for which the authors are grateful.

Conflict of interest

The authors declare no conflicts of interest relevant to this article.

References

Achamo, T. and Yadav, O. P. (2016). Removal of 4-Nitrophenol from water using Ag-NP-tridoped TiO_2 by photocatalytic oxidation technique Ubertas Academica. Analytic Al Chemistry Insights, **11**:ACI-S31508.

Aggarwal, P.; Singh, S.; Sangwan, S.; Moond, M. and Devi, P. (2022). Effect of extraction solvents on antioxidant potential of *Prosopis cineraria* (L.) leaves. Ann. Phytomed., **11**:426-431.

Awad, M.A.; Hendi, A.A.; Ortashi, K.M.; Alzahrani, B.; Soliman, D.; Alanazi, A.; Alenazi, W.; Taha, R.M.; Ramadan, R.; El-Tohamy, M. and AlMasoud, N. (2021). Biogenic synthesis of silver nanoparticles using *Trigonella foenum-graecum* seed extract: Characterization, photocatalytic and antibacterial activities. Sensors and Actuators A: Physical, **323**:112670.

Bahuguna, G.; Kumar, A.; Mishra, N. K.; Kumar, C.; Bahlwal, A.; Chaudhary, P. and Singh, R. (2016). Green synthesis and characterization of silver nanoparticles using aqueous petal extract of the medicinal plant *Combretum indicum*. Materials Research Express, **3**(7):075003.

Chen, T.; Pourmand, M.; Feizpour, A.; Cushman, B. and Reinhard, B. M. (2013). Tailoring plasmon coupling in self-assembled one-dimensional Au nanoparticle chains through simultaneous control of size and gap separation. The Journal of Physical Chemistry Letters, **4**(13):2147-2152.

Chen, X.; Zhao, D.; An, Y.; Zhang, Y.; Cheng, J.; Wang, B. and Shi, L. (2008). Formation and catalytic activity of spherical composites with surfaces coated with gold nanoparticles. Journal of Colloid and Interface Science, **322**(2):414-420.

Dalal, R.; Singh, S.; Sangwan, S.; Moond, M. and Beniwal, R. (2022). Biochemical and molecular mechanism of plant-mediated synthesis of silver nanoparticles: A review. Mini-Reviews in Organic Chemistry, **19**(8):939-954.

Deka, P.; Bhattacharjee, D.; Sarmah, P.; Deka, R. C. and Bharali, P. (2017). Catalytic reduction of water contaminant '4-nitrophenol'over manganese oxide supported Ni nanoparticles. Trends in Asian Water Environmental Science and Technology, **17**:35-48.

Deshmukh, A. R.; Gupta, A. and Kim, B. S. (2019). Ultrasound assisted green synthesis of silver and iron oxide nanoparticles using fenugreek seed extract and their enhanced antibacterial and antioxidant activities. Bio. Med. Research International, **19**:1-14.

Devi, D.; Singh, S.; Moond, M.; Matoria, P.; Kumari, S.; Saini, K. and Sharma R.K. (2023). Phytochemical analysis and antioxidant potential of *Albizia lebbeck* (L.) seeds. Ann. Phytomed.; **12**(1):502-507.

Devi, R.; Singh, S.; Sangwan, S.; Moond, M.; Kakkar, S.; Sharma, R.K. and Kumar, S. (2024). Phytomediated fabrication of silver nanoparticles using *Syzygium cumini* L. aqueous leaf extract and evaluation of their antioxidant potential. Ann. Phytomed.; **13**(1):1-8.

Jain, S. and Mehata, M. S. (2017). Medicinal plant leaf extract and pure flavonoid mediated green synthesis of silver nanoparticles and their enhanced antibacterial property. Scientific Reports, **7**(1):1-13.

Kastner, C. and Thunemann, A. F. (2016). Catalytic reduction of 4-nitrophenol using silver nanoparticles with adjustable activity. Langmuir, **32**(29): 7383-7391.

Kong, X.; Zhu, H.; Chen, C.; Huang, G. and Chen, Q. (2017). Insights into the reduction of 4-nitrophenol to 4-aminophenol on catalysts. Chemical Physics Letters, **684**:148-152.

Kumar, B.; Angulo, Y.; Smita, K.; Cumbal, L. and Debut, A. (2016). Capuli cherry-mediated green synthesis of silver nanoparticles under white solar and blue LED light. Particuology, **24**:123-128.

Lee, S. H. and Jun, B. H. (2019). Silver nanoparticles: Synthesis and application for nanomedicine. International Journal of Molecular Sciences, **20**(4):865.

Mahiuddin, M.; Saha, P. and Bungo, O. (2020). Green synthesis and catalytic activity of silver nanoparticles based on *Piper chaba* stem extracts. Nanomaterials, **10**(9):1777.

Makarov, V.V.; Love, A.J.; Sinitsyna, O.V.; Makarova, S.S.; Yaminsky, I.V.; Taliansky, M.E. and Kalinina, N.O. (2014). "Green" nanotechnologies: synthesis of metal nanoparticles using plants. Acta Naturae, **6**(1):20-27.

Marcelo, G.; Muñoz-Bonilla, A. and Fernández-García, M. (2012). Magnetite–polypeptide hybrid materials decorated with gold nanoparticles: study of their catalytic activity in 4-nitrophenol reduction. The Journal of Physical Chemistry C, **116**(46):24717-24725.

Mejia, Y. R. and Bogireddy, N. K. R. (2022). Reduction of 4-nitrophenol using green-fabricated metal nanoparticles. RSC advances, **12**(29):18661-18675.

Moond, M.; Singh, S.; Devi, R.; Beniwal, R.; Matoria, P.; Kumari, S. and Sharma, R. K. (2023). Proximate and mineral analysis of *Trigonella foenum-graecum* L. (Fenugreek) seeds and leaves of variety HM444. Ann. Phytomed.; **12**(1):546-552.

Moond, M.; Singh, S.; Devi, R.; Pinki and Rajita (2023). Estimation of phytochemicals and antioxidant potency of *Trigonella foenum-graecum* leaves (Variety HM444). Agricultural Science Digest. doi:10.18805/ag. D-5677.

Moond, M.; Singh, S.; Sangwan, S.; Devi, P.; Beniwal, A.; Rani, J.; Kumari, A. and Rani, S. (2023). Biosynthesis of silver nanoparticles utilizing leaf extract of *Trigonella foenum-graecum* L. for catalytic dyes degradation and colorimetric sensing of Fe^{3+}/Hg^{2+}. Molecules, **28**(3):951.

Moond, M.; Singh, S.; Sangwan, S.; Devi, R. and Beniwal, R. (2022). Green synthesis and applications of silver nanoparticles: A systematic review. AATCC Journal of Research, **9**(6):272-85.

Moond, M.; Singh, S.; Sangwan, S.; Devi, R.; Rani, J.; Beniwal, A. and Beniwal, R. (2023). Synthesis, optimization and characterization of Silver nanoparticles using aqueous seed extract of *Trigonella foenum graceum* L. for catalytic reduction of p nitrophenol. Chemistry Select, **8**(29): e202301006.

Moond, M.; Singh, S.; Sangwan, S.; Rani, J.; Beniwal, A.; Matoria, P.; Saini, K. and Sharma, R. K. (2023). Proximate composition, phytochemical analysis and antioxidant potency of *Trigonella foenum-graecum* L. seeds. Ann. Phytomed.; **12**(1):486-491.

Moond, M.; Singh, S.; Sangwan, S.; Rani, S.; Beniwal, A.; Rani, J.; Kumari, A.; Rani, I. and Devi, P. (2023). Phytofabrication of silver nanoparticles using *Trigonella foenum-graceum* L. leaf and evaluation of its antimicrobial and antioxidant activities. International Journal of Molecular Sciences, **24**(4):3480.

Pei, X.; Qu, Y.; Shen, W.; Li, H.; Zhang, X.; Li, S.; Zhang, Z. and Li, X. (2017). Green synthesis of gold nanoparticles using fungus *Mariannaea* sp. HJ and their catalysis in reduction of 4-nitrophenol. Environmental Science and Pollution Research, **24**:21649-21659.

Poonam, Singh, S.; Moond, M.; Sangwan, S. and Devi, P. (2023). Phytochemicals and antioxidant potential of *Andrographis paniculata* (Burm. f.)Wall. ex Nees. Ann. Phytomed.;**12**(2):769-775.

Rizwana, H.; Alwhibi, M.S.; Aldarsone, H.A.; Awad, M.A.; Soliman, D.A. and Bhat, R.S. (2021). Green synthesis, characterization and antimicrobial activity of silver nanoparticles prepared using *Trigonella foenum-graecum* L. leaves grown in Saudi Arabia. Green Processing and Synthesis, **10**(1):421-429.

Samari, F.; Salehipoor, H.; Eftekhar, E. and Yousefinejad, S. (2018). Low-temperature biosynthesis of silver nanoparticles using mango leaf extract: Catalytic effect, antioxidant properties, anticancer activity and application for colorimetric sensing. New Journal of Chemistry, **42**(19):15905-15916.

Sathishkumar, M.; Sneha, K. and Yun, Y.S. (2010). Immobilization of silver nanoparticles synthesized using *Curcuma longa* tuber powder and extract on cotton cloth for bactericidal activity. Bioresource Technology, **101**(20): 7958-7965.

Sen, I. K.; Maity, K. and Islam, S. S. (2013). Green synthesis of gold nanoparticles using a glucan of an edible mushroom and study of catalytic activity. Carbohydrate Polymers, **91**(2):518-528.

Singh, J.; Mehta, A.; Rawat, M. and Basu, S. (2018). Green synthesis of silver nanoparticles using sun dried tulsi leaves and its catalytic application for 4-Nitrophenol reduction. Journal of Environmental Chemical Engineering, **6**(1):1468-1474.

Singh, R.P.; Magesh, S. and Rakkiyappan, C. (2011). Formation of Fenugreek (*Trigonella foenum-graecum* extract mediated Ag nanoparticles: mechanism and applications. International Journal of Bio-Engineering Sciences and Technology, **2**(3):70-80.

Singh, S.; Sangwan, S.; Sharma, P.; Devi, P. and Moond, M. (2021). Nanotechnology for sustainable agriculture: An emerging perspective. Journal of Nanoscience and Nanotechnology, **21**(6):3453-3465.

Sooraj, M. P.; Nair, A. S. and Vineetha, D. J. C. P. (2021). Sunlight-mediated green synthesis of silver nanoparticles using *Sida retusa* leaf extract and assessment of its antimicrobial and catalytic activities. Chemical Papers, **75**(1):351-363.

Umadevi, M.; Bindhu, M. R. and Sathe, V. (2013). A novel synthesis of malic acid capped silver nanoparticles using *Solanum lycopersicums* fruit extract. Journal of Materials Science and Technology, **29**(4):317-322.

Citation **Monika Moond, Sushila Singh, Seema Sangwan and Rajni Kant Sharma (2024). Catalytic degradation of organic pollutant by biosynthesized silver nanoparticles using *Trigonella foenum-graceum* L. leaves. Ann. Phytomed., 13(1):1259-1269. http://dx.doi.org/10.54085/ap.2024.13.1.137.**